

# Study of the aberrations of the IMP heavy ion microbeam irradiation system<sup>\*</sup>

SHENG Li-Na(盛丽娜)<sup>1,2;1)</sup> SONG Ming-Tao(宋明涛)<sup>1</sup> GAO Da-Qing(高大庆)<sup>1</sup>  
HE Yuan(何源)<sup>1</sup> ZHANG Bin(张斌)<sup>1</sup> ZHANG Xiao-Qi(张小奇)<sup>1</sup>

1 (Institute of Modern Physics, Chinese Academy of Sciences, P.O. Box 31, 509 Nanchang Rd. Lanzhou 730000, China)

2 (Graduate University of Chinese Academy of Sciences, Beijing 100086, China)

**Abstract** A high energy heavy ion microbeam irradiation system is constructed at the Institute of Modern Physics (IMP) of the Chinese Academy of Sciences (CAS). A quadrupole focusing system, in combination with a series of slits, has been designed here. The IMP microbeam system is described in detail. The intrinsic and parasitic aberrations associated with the magnets are simulated. The ion beam optics of this microbeam system is investigated systematically. Then the optimized initial beam parameters are given for high spatial resolution and high hitting rates.

**Key words** microbeam, high energy, ion beam optics, aberration

**PACS** 41.85.Gy

## 1 Introduction

An ion microbeam system is a powerful tool for analytical applications in material and biology research at micron scale. At present, there are two ways to form the microbeam: collimating by collimators and focusing by quadrupole magnets. With the demand of better spatial resolution in beam spot size, focusing by quadrupole magnets is more and more popular. Consequently, the quadrupole magnets cause aberrations inevitably which make the beam spot size broaden and deform, which will affect the beam quality seriously.

The early systematic investigation of the aberration is by G.W. Grime and F. Watt<sup>[1]</sup>. Matrix methods and numerical ray-tracing are the two techniques to calculate the beam optics of the charged particles<sup>[2]</sup>. The extensively used computer programs to simulate the beam optics are TRANSPORT<sup>[3]</sup>, TRAX, TURTLE, Zgoubi, Geant4<sup>[4]</sup>, MULE, PRAM. MULE can only calculate the beam optics to the first order. PRAM, Geant4 and TRAX are generally used to simulate the straight beam line. Zgoubi needs to

input the real field distribution. TRANSPORT and TURTLE can calculate to the third order and simulate the bending beam line.

The ion beam optical property for the IMP microbeam system is calculated with 80 MeV/u C<sup>6+</sup> ions by computer codes MULE and TRANSPORT. All the simulations in this paper begin with the object slit.

## 2 The IMP microbeam line

The IMP high energy heavy ion microbeam system is based on the Heavy Ion Research Facility in Lanzhou (HIRFL). The characteristic of this system is the vertical irradiation and the high energy up to 100 MeV/u for C ions. A high precision quadrupole triplet is adopted in the design. The schematic of the IMP microbeam system is shown in Fig. 1<sup>[5]</sup>. The ions enter the microbeam end-station after two dipole magnets (R1B1 and R0B0) with 50° and 30° respectively. Then the ions pass through three quadrupole magnets (R0Q1-R0Q3) with a bore diameter of 80 mm to be focused at the object slit.

Received 6 January 2009

<sup>\*</sup> Supported by Development of the Key Equipment for Research of CAS (0713040YZ0)

1) E-mail: shenglina@impcas.ac.cn

©2009 Chinese Physical Society and the Institute of High Energy Physics of the Chinese Academy of Sciences and the Institute of Modern Physics of the Chinese Academy of Sciences and IOP Publishing Ltd

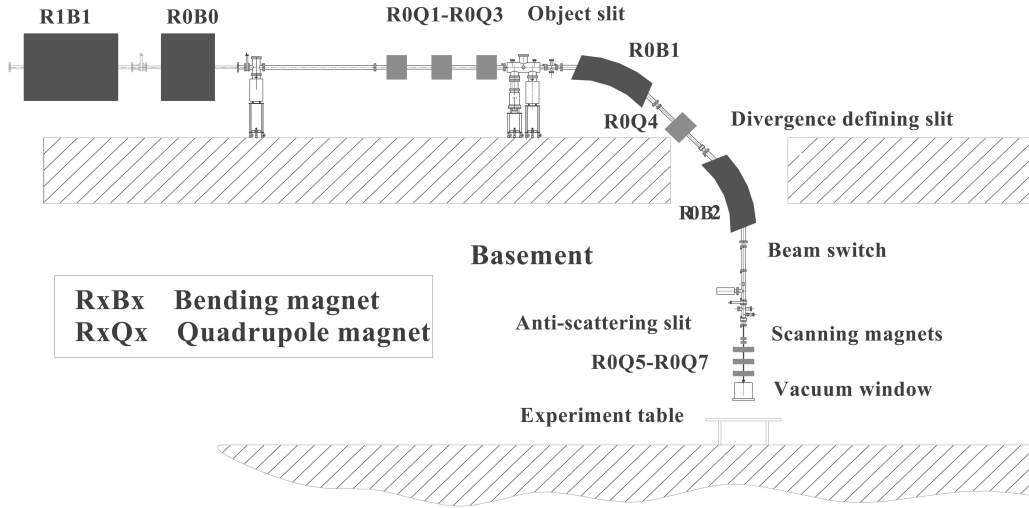


Fig. 1. Schematic of the IMP microbeam system.

The object slit with an aperture 0–150  $\mu\text{m}$  and the following two slits are all made by Technisches Büro S. Fischer. A symmetrically achromatic system, composed of two identical  $45^\circ$  dipole magnets (R0B1 and R0B2) and a quadrupole magnet R0Q4, guides the beam downwards. A divergence defining slit, defining the divergence angle and the momentum spread of the beam simultaneously, is set before R0B2. The two dipole magnets and the divergence defining slit make an energy analyzer. At last, the ion beam is strongly focused to 1  $\mu\text{m}$  on the target by a high gradient quadrupole triplet (R0Q5-R0Q7) with a bore diameter of 15 mm and a maximum pole field of 1.0 T. The anti-scattering slit, set before the quadrupole triplet, prevents those scattered ions from entering the quadrupole triplet. A silicon nitride vacuum window at the end of beam line is used to extract the beam into the air to irradiate living cells and detect the secondary electron<sup>[6]</sup>. The hits of ions are controlled by the electrostatic deflector plates (beam switch) associated with the secondary electron detector. A 2-D ion scanning system is used for spot scanning or raster scanning.

### 3 Calculation of ion beam optics

#### 3.1 Intrinsic aberrations

The magnetic quadrupole triplet is the key part of the IMP microbeams, arranged in either CDC (converging-diverging-converging) or DCD (diverging-converging-diverging) configuration. Note that, the results in Table 3 are calculated by CDC configuration. The magnetic focusing system creates a demagnified image of the object aperture in

the image plane, and also suffers from intrinsic and parasitic aberrations which broaden the beam spot. There are three dominant types of aberrations in a quadrupole focusing system<sup>[7]</sup>: chromatic aberration (due to the beam momentum spread), spherical aberration (caused by fringe quadrupole field effects) and parasitic aberration (due to mechanical imperfections in the lenses or the system). The final beam spot size depends strongly on the demagnification factor and the correction of these aberrations in the focusing system, which can be shown by the expression of the position of an ion in a focusing microbeam system<sup>[8]</sup>,

$$x_i = \langle x|x \rangle x_o + \langle x|\theta \rangle \theta_o + \langle x|\theta\delta \rangle \theta_o \delta_o + \langle x|\theta^3 \rangle \theta_o^3 + \langle x|\theta^2 \rangle \theta_o \Phi_o^2 + \dots, \quad (1)$$

$$y_i = \langle y|y \rangle y_o + \langle y|\Phi \rangle \Phi_o + \langle y|\Phi\delta \rangle \Phi_o \delta_o + \langle y|\Phi^3 \rangle \Phi_o^3 + \langle y|\theta^2\Phi \rangle \theta_o^2 \Phi_o + \dots, \quad (2)$$

where  $(x_o, \theta_o, y_o, \Phi_o)$  represents the position and divergence angle of a beam particle in the object plane,  $\delta_o$  is the particle momentum relative to the mean momentum, the demagnification of the system is  $\langle x|x \rangle^{-1}$  and  $\langle y|y \rangle^{-1}$  in the image plane,  $\langle x|\theta \rangle$  and  $\langle y|\Phi \rangle$  are the astigmatism coefficients,  $\langle x|\theta\delta \rangle$  and  $\langle y|\Phi\delta \rangle$  are the chromatic aberration coefficients, and  $\langle x|\theta^3 \rangle$ ,  $\langle x|\theta\Phi^2 \rangle$ ,  $\langle y|\Phi^3 \rangle$  and  $\langle y|\theta^2\Phi \rangle$  are the spherical aberration coefficients (Fig. 2). In a well-focused system, the astigmatism coefficients are zero.

Some physical parameters and the dominant aberration coefficients for the IMP microbeam system as calculated by TRANSPORT and MULE codes are shown in Table 1. The figure of merit of the system<sup>[9]</sup>, Q factor, is also given. This factor which combines the demagnifications and spherical aberration terms

is defined as follows. Usually, a system with a large value of  $Q$  potentially offers superior performance.

$$Q = \frac{D_x \cdot D_y}{\sqrt[3]{\langle x|\theta^3 \rangle \cdot \langle y|\phi^3 \rangle}}. \quad (3)$$

Many other calculations were also made but not listed here to illustrate the variation of the final beam spot size with the object sizes and the divergence angles. From those calculations, two conclusions can be drawn. First, the beam spot size is rising linearly whatever first order or third order with the increase of the object size, but  $x_i$  for the third order is more sensitive than  $y_i$  to the change in object size. Second, the divergence angles have no effect on the beam spot size for the first order but more effects for the third order. In addition, the divergence  $\theta_0$  contributes to  $x_i$  and  $y_i$  for third order, which is similar to  $\Phi_0$ .

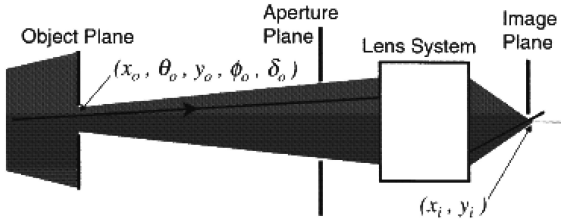


Fig. 2. Designation of the object ray vector and its corresponding coordinates in the image plane<sup>[8]</sup>.

Table 1. Beam optical parameters for the IMP CDC and DCD configurations.

|   | IMP(CDC)        | IMP(DCD)        |
|---|-----------------|-----------------|
| ion species   | C <sup>6+</sup> | C <sup>6+</sup> |
| energy/MeV  | 960             | 960             |
| $D_x$   | 15.19           | 16.07           |
| $D_y$   | -15.20          | -17.37          |
| chromatic aberration coefficients ( $\mu\text{m}/(\text{mrad}\%)$ ) |                 |                 |
| $\langle x \theta\delta \rangle$                                    | -329.7          | -129.6          |
| $\langle y \Phi\delta \rangle$                                      | 182.0           | 443.2           |
| spherical aberration coefficients ( $\mu\text{m}/\text{mrad}^3$ )   |                 |                 |
| $\langle x \theta^3 \rangle$  | 175.1           | 16.89           |
| $\langle x \theta\Phi^2 \rangle$                                    | 166.0           | 188.0           |
| $\langle y \Phi^3 \rangle$  | -33.71          | -378.8          |
| $\langle y \theta^2\Phi \rangle$                                    | -165.9          | -173.9          |
| figure of merit $Q$   | 12.78           | 15.04           |

Suppression of focusing errors, induced by spherical and chromatic aberrations in the quadrupole focusing system, is very significant for the microbeam production. Precise fabrication and alignment of the magnets are required for the suppression of spherical aberrations. Minimization of the momentum spread of the beam is essential to reduce the chromatic aberrations. Table 2 shows the simulations for the opti-

mized initial beam parameters to attain 1  $\mu\text{m}$  beam spot in vacuum chamber.

Table 2. Optimized initial beam parameters for CDC and DCD configurations.

| initial beam parameters | CDC configuration | DCD configuration |
|-------------------------|-------------------|-------------------|
| $x_0$                   | 7 $\mu\text{m}$   | 7 $\mu\text{m}$   |
| $y_0$                   | 7 $\mu\text{m}$   | 7 $\mu\text{m}$   |
| $\theta_0$              | 0.05 mrad         | 0.1 mrad          |
| $\Phi_0$                | 0.1 mrad          | 0.05 mrad         |
| $\delta_0$              | 0.008%            | 0.016%            |

### 3.2 Parasitic aberrations

The minimum spot size achieved in a quadrupole system is influenced strongly by parasitic aberrations due to the imperfections in the construction and misalignment of the instruments. The misalignment contains a quadrupole transverse translations  $U$ ,  $V$ , tilts  $\alpha$ ,  $\beta$  around  $y$  and  $x$  axis, rotation  $\rho$  around the beam optical axis and percentage change  $\varepsilon$  in the excitation<sup>[1]</sup>. To minimize the influence of parasitic aberrations, some measures were taken, such as the one-piece magnet poles and yoke were cut as one body from a single iron piece using a numerically controlled machine, every four pole tips are all cut with an accuracy of micron scale, the three quadrupoles were fabricated into a monobloc triplet and treated as a whole in the misalignment simulation. Some plots have been drawn but not shown here to get the trend of the final beam spot size against the misalignment of the triplet and the predictions of the parasitic aberration coefficients for the IMP microbeams with displacement on target less than 100 nm (Table 3). It appears that a minimum precision for the monobloc

Table 3. Parasitic aberration coefficients of the monobloc triplet of the IMP microbeam system.

|   | coefficient                         | precision           |
|---|-------------------------------------|---------------------|
| $D_x$                                   | 15.19                               | -                   |
| $D_y$                                   | -15.20                              | -                   |
| $\langle x U \rangle$                   | 0.32 $\mu\text{m}/\mu\text{m}$      | 0.25 $\mu\text{m}$  |
| $\langle y V \rangle$                   | 0.32 $\mu\text{m}/\mu\text{m}$      | 0.25 $\mu\text{m}$  |
| $\langle x \alpha \rangle$              | 62.50 $\mu\text{m}/\text{mrad}$     | 1.6 $\mu\text{rad}$ |
| $\langle y \beta \rangle$               | 111.11 $\mu\text{m}/\text{mrad}$    | 0.9 $\mu\text{rad}$ |
| $\langle x \Phi\rho \rangle$            | 0.45 $\mu\text{m}/\text{mrad}^2$    | 2.0 mrad            |
| $\langle y \theta\rho \rangle$          | 0.40 $\mu\text{m}/\text{mrad}^2$    | 4.0 mrad            |
| $\langle x \theta\varepsilon_1 \rangle$ | 40.00 $\mu\text{m}/\text{mrad}\%$   | 0.04%               |
| $\langle x \theta\varepsilon_2 \rangle$ | -160.00 $\mu\text{m}/\text{mrad}\%$ | -0.01%              |
| $\langle x \theta\varepsilon_3 \rangle$ | -28.57 $\mu\text{m}/\text{mrad}\%$  | -0.07%              |
| $\langle y \Phi\varepsilon_1 \rangle$   | 53.33 $\mu\text{m}/\text{mrad}\%$   | 0.015%              |
| $\langle y \Phi\varepsilon_2 \rangle$   | -32.00 $\mu\text{m}/\text{mrad}\%$  | -0.025%             |
| $\langle y \Phi\varepsilon_3 \rangle$   | 20.00 $\mu\text{m}/\text{mrad}\%$   | 0.04%               |

triplet of  $0.25\ \mu\text{m}$  in transverse translations ( $U, V$ ) or  $0.0009\ \text{mrad}$  in tilts ( $\alpha, \beta$ ) is required as well as a field tolerance of  $10^{-4}$ .

## 4 Discussions

The final image can be further improved by reducing the object slit and the divergence defining slit at the cost of fewer particles. Though the chromatic aberrations have more influences than the spherical aberrations on the final beam spot size, there's no necessity to use sextupoles to correct the second order aberrations owing to the energy analyzer. The beam positioning is very sensitive to the stability of the two dipole magnets. To minimize the displacement of the beam centroid, a tolerance of  $10^{-5}$  is required for the power supply of the dipoles. Besides, the field tolerance of  $10^{-3}$  for the quadrupole between the two

dipole magnets is enough for this microbeam.

## 5 Conclusions

The calculated aberrations of the IMP microbeam system are proved to be reasonable after comparing it with that of other existing microbeam facilities. It is believed that these calculations would guide the installation, alignment and tuning of the IMP microbeam system. Now the ray-tracing for the IMP microbeam system with the Zgoubi code is studied, and its results will be compared with that calculated above.

Now all the magnetic elements are well prepared to be installed. Some elemental measurements will be made to test the final beam profile and the targeting accuracy, which will verify the above discussions.

---

## References

- 1 Grime G W, Watt F. Beam Optics of Quadrupole Probing Systems. Bristol: Adam Hilger Ltd, 1984
- 2 Grime G W, Watt F, Blower G D et al. Nucl. Instrum. Methods, 1982, **197**: 97—109
- 3 Gillespie G H, Hill B W, Brown N A et al. [www.ghga.com/accelsoft/pbolab.html](http://www.ghga.com/accelsoft/pbolab.html)
- 4 Agostinelli S et al. Nucl. Instrum. Methods A, 2003, **506**: 250—303 Available from: <http://geant4.web.cern.ch/geant4/>
- 5 SONG Ming-Tao, SHENG Li-Na, WANG Zhi-Guang et al. Chinese Physics C, 2008, **32**(Sup I): 259—261
- 6 SHENG Li-Na, SONG Ming-Tao, LIU Jie. Chinese Physics C, 2008, **32**(Sup I): 74—76
- 7 Mutsaers P H A. Nucl. Instrum. Methods B, 1996, **113**: 323—329
- 8 Jamieson D N. Nucl. Instrum. Methods B, 2001, **181**: 1—11
- 9 Jamieson D N, Rout B, Szymanski R et al. Nucl. Instrum. Methods B, 2002, **181**: 54—59